DOI 10.1007/s11182-019-01658-3

Russian Physics Journal, Vol. 61, No. 12, April, 2019 (Russian Original No. 12, December, 2018)

STRUCTURE AND PHASE COMPOSITION OF HEAT-RESISTANT Ni–Al–Co ALLOY AFTER ANNEALING AND CREEP

N. A. Koneva,[1] A. I. Potekaev,[2,3] E. L. Nikonenko,[1] N. A. Popova,[1] A. A. Klopotov,[1,2] and V. D. Klopotov[4]

UDC 539.2

The paper presents research into the structure and phase composition of Ni–Al–Co *alloy modified by rhenium (~3 at.%) alloying. Observations are carried out using the transmission electron microscopy. The initial state of the alloy is the state after the directional crystallization. The alloy is further subjected to 900°C annealing during 1143 h. Creep tests are additionally carried out for this alloy at the same temperature and time and 400 MPa load. It is shown that FCC disordered γ- and ordered γ′-phases are major in all alloy states. Secondary phases are found to be σ-phase, χ-phase, Laves and* $AlRe_2$ *phases. Experiments show that the high temperature annealing changes the phase composition of the alloy. Thus, the amount of the ordered γ′-phase increases, while that of disordered γ-phase decreases. During the creep process, the amount of the former reduces and the amount of the latter increases. The annealing process modifies the phase composition in secondary phases. It is found that the structural modification caused by the creep process differs from that caused by the annealing process. Thus, the creep-induced modification of the cuboid structure in γ′-phase is stronger than due to annealing. Dislocations are observed in γ- and γ′-phases in all states of the alloy. During the annealing process, the dislocation density in γ-phase is higher than in γ′-phase, and vice versa during the creep process. The experiments show that the behavior of the dislocation structures is different during the annealing and creep processes.*

Keywords: heat-resistant alloy, structure and phase composition, rhenium, high-temperature effect, dislocation, annealing, creep.

INTRODUCTION

The properties of heat-resistant nickel alloys are determined by the thermal stability of their structure, size, shape and the amount of the strengthening γ′-phase and strength properties of γ-phase solid solution [1–4]. Physicochemical properties of these alloys can be improved by the traditional alloying. The latest-generation alloys can be modified by the refractory alloying elements, such as Cr, Mo, W, Ta, Re and others. Such alloying provides the increase in the working temperature due to the high melting temperature of the phases formed [5–10]. For example, rhenium as well as other refractory elements is an active phase-forming element. To the author's knowledge, the composition and localization of phases forming in these superalloys after the use of these alloying elements have been scarcely investigated.

[1]Tomsk State University of Architecture and Building, Tomsk, Russia, e-mail: koneva@tsuab.ru; vilatomsk@mail.ru; natalya-popova-44@mail.ru; klopotovaa@tsuab.ru; [2]National Research Tomsk State University, Tomsk, Russia; [3]V. D. Kuznetsov Siberian Physical-Technical Institute at National Research Tomsk State University, Tomsk, Russia, e-mail: kanc@spti.tsu.ru; [4]National Research Tomsk Polytechnic University, Tomsk, Russia, e-mail: vdklopotov@mail.ru. Translated from Izvestiya Vysshikh Uchebnykh Zavedenii, Fizika, No. 12, pp. 65–71, December, 2018. Original article submitted August 14, 2018.

Such superalloys nearly loss stability under thermal loading. In these cases, a range of the low-stable and metastable structures and phases appears in superalloys. Therefore, it is important to study the initial structure and phase composition of superalloys after alloying by both ultrafine refractory powders and refractory metals.

It is interesting to note that the low-stable and unstable regions in the crystal lattice before phase transformations are well observed in a wide range of metals and alloys [11–21].

In order to achieve the required functional properties of these alloys, it is expedient to study changes in the structure and phase composition after their alloying. Importantly, a study of processes induced by Cr, Ta and Re alloying elements should include investigations of the fine structure of superalloys. Such investigations will show the modified structure and phase composition, microstructure and the formation of secondary phases in superalloys.

The aim of this work is to investigate the structure and phase composition of Re-alloyed heat-resistant Ni–Al–Co alloy in the initial state and annealed and crept states.

MATERIALS AND METHODS

Ni-Al-Co superalloy was investigated in this experiment. Its composition included 69–59 at.% Ni, 12–15 at.% Al and 10–13 at.% Co. Cr, Ta and Re alloying elements were used in the amount of not over 3.5 at.% each, and W and Mo alloying elements were used in a lower content.

Thin foils were obtained from plates using electroerosion cutting with their plane normal to the specimen axis. Three states of the alloy structure were examined, namely:

1) the initial state, after the direct crystallization;

2) after 900°C annealing for 1143 hours;

3) after creep tests at 900°C for 1143 hours and 400 MPa load.

The alloy plates of different thickness were obtained from the ingot on an electrospark discharge machine using the soft operating mode that did not induce distortions or additional defects in the material. The alloy plates were cut perpendicular to <001> direction of the crystal growth. The microstructure and phase composition of the specimens were investigated on a transmission electron microscope (TEM) EM-125 at 125 kV accelerating voltage and 25000× magnification. TEM observations included electrolytic polishing of the alloy in an oversaturated solution of chromic anhydride containing orthophosphoric acid. Medium sizes of the structural elements and parameters of the fine structure were detected on micrographs using the secant method [6, 7]. All the experimental data were statistically processed. The phase analysis used the TEM images confirmed by the micro-diffraction patterns [8] and bright- and dark-field images obtained in the respective reflections [6].

EXPERIMENTAL RESULTS

Let us consider the phase composition, morphology and dislocation structures forming at different temperatures.

Phase composition and morphology

Major γ′- and γ-phases in the volume of ~0.99 observed in all alloy states are given Table 1 [3, 6, 8]. The volume of secondary phases is not over 0.01.

Now we describe in detail the observed phases and their morphology.

1) γ′-phase is the FCC solid solution with $L1_2$ structure [3, 6, 7, 9, 22–25]. The morphology of this phase represents spheroidized and clear faceted cuboids. These cuboids have an isotropic shape in the original state of the alloy. After annealing, cuboids acquire anisotropic shape and became clear faceted. After the creep process, spheroidized cuboids are observed in each alloy state. TEM images of γ′-phase are shown in Fig. 1.

TABLE 1. Volume Fractions of Phases

Alloy states	γ′-phase, %	γ-phase, %	Secondary phases
Initial state, after the direct crystallization	80.0	19.7	χ-phase
After 900°C annealing for 1143 h	83.0	16.5	$AlRe_2$
Post-creep state (900°C creep for 1143 h and 400 MPa load)	69.0	30.8	Laves phase σ-phase

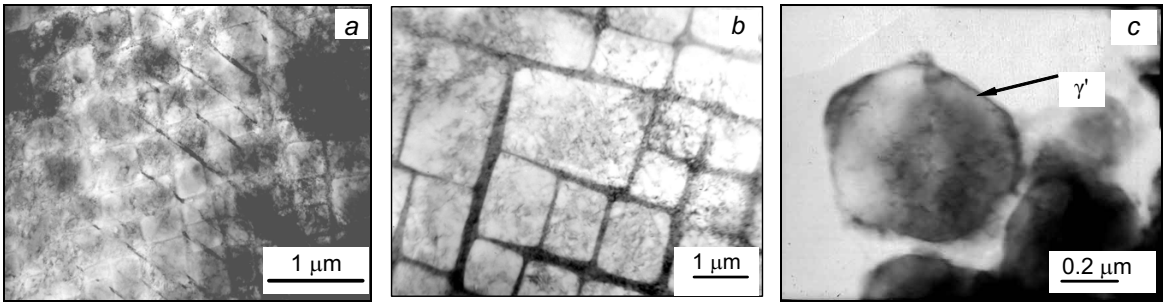

Fig. 1. TEM images of γ′-phase: *a* – clear faceted isotropic cuboids (initial state); *b* – clear faceted anisotropic cuboids (900°C annealing for 1143 h); *c* – spheroidized cuboids (creep at 900°C annealing for 1143 h)

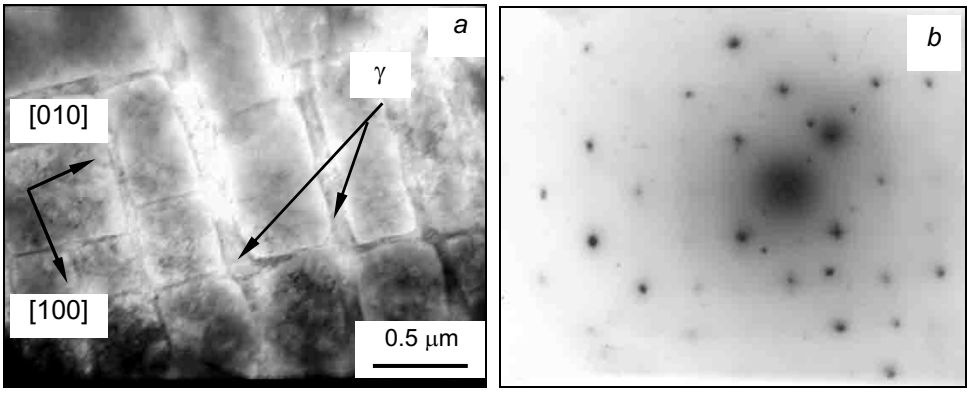

Fig. 2. TEM images of the alloy structure after 900°C annealing for 1143 h: *a* – bright-field image; *b* – microdiffraction pattern of the region (*a*). Black arrows indicate γ-phase layers.

2) γ-phase is the disordered FCC solid solution. The morphology of this phase represents thin layers between cuboids of γ′-phase as shown in Fig. 2. Although γ-phase is observed in the alloy in rather a small amount, it is a major phase [3, 6–9].

3) χ-phase ($TaRe_x$) is an electron compound of transition metals with a complex BCC structure. This phase represents rounded particles located in cuboids of γ′-phase [6–8]. TEM images of χ-phase and its microdiffraction pattern are shown in Fig. 3.

4) σ-phase represents a multicomponent solid solution with the tetragonal crystal structure having a $P4_2/mnm$ space group (FeCr type). There are such elements as Re, Cr, Ta, W, Mo, Ni, Co and Al [6, 7, 10, 26, 27] in this phase. σ-phase has an acicular shape, an example of which is presented in Fig. 4.

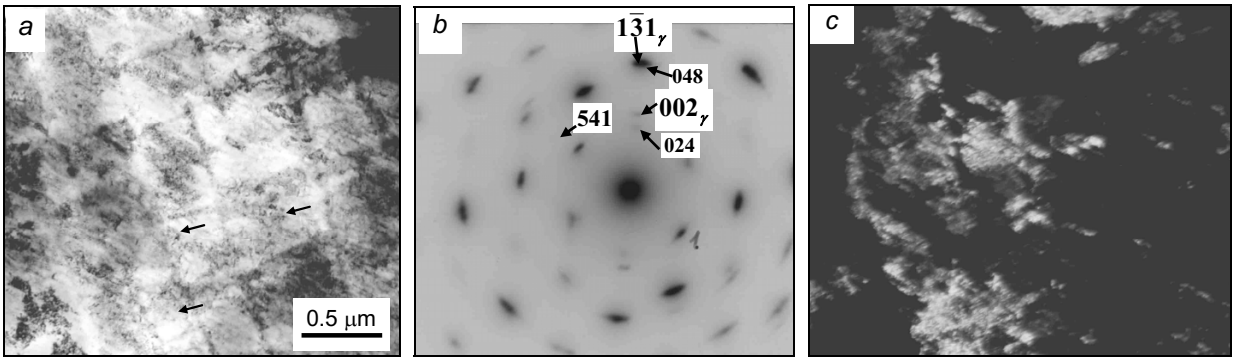

Fig. 3. TEM images of the alloy structure in the initial state: *a* – bright-field image; *b* – microdiffraction pattern; *c* – dark-field image of $\left[\bar{1}31\right]$ γ and [048] matching reflections of χ-phase. Black arrows indicate χ-phase particles.

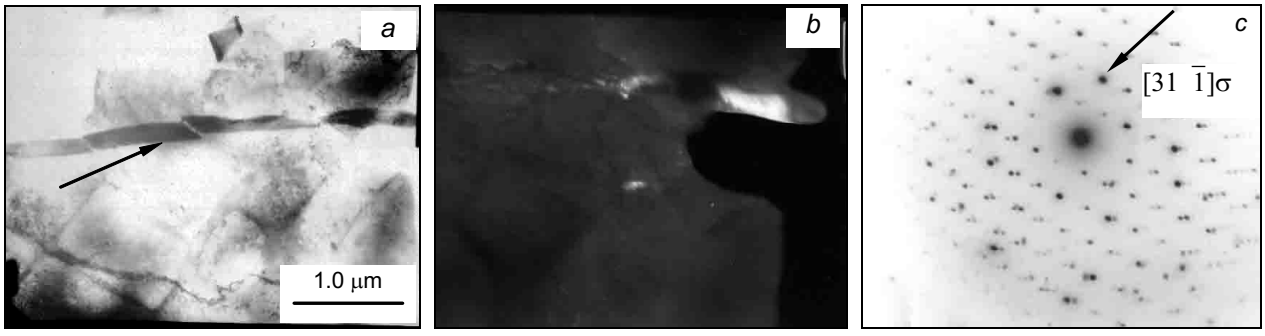

Fig. 4. TEM images of the annealed alloy structure: *a* – acicular formations (indicated with black arrow); *b* – dark-field image in [31 $\bar{1}$] reflection indicated by the black arrow (*c*).

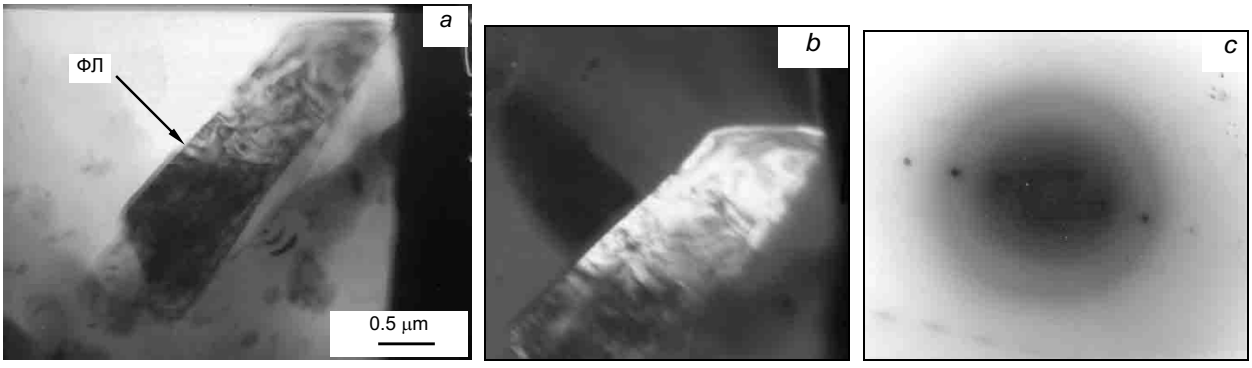

Fig. 5. TEM images of Laves phase: *a* – bright-field image of lamellar formation (indicated with black arrow); *b* – dark-field image; *c* – microdiffraction pattern of the region (*a*).

5) The cubic Laves phase is characterized by the space group $Fd\bar{3}m$ and the crystal structure of $MgCu_2$ type [6–8]. This phase is observed in γ-phase and represents lamellar anisotropic formations. Their average size is about ~0.5×2.5 μm (Fig. 5). Laves phase has no effect on morphology of γ′- and γ-phases and does not disturb their distribution in the alloy

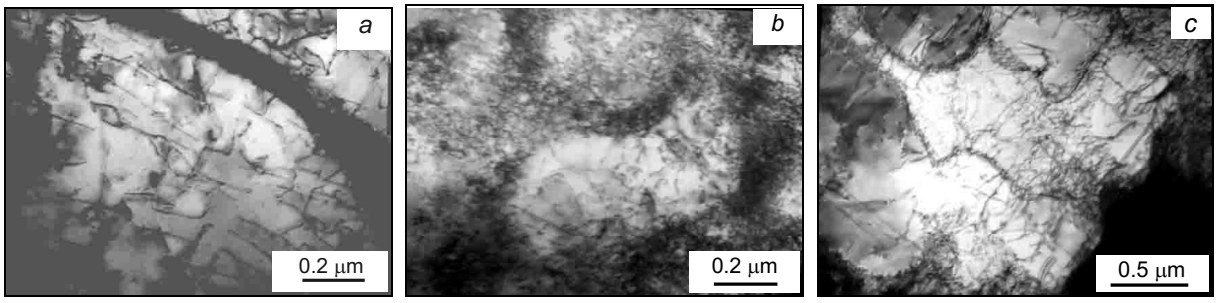

Fig. 6. TEM images of dislocation substructures: *a* – network; *b* – cell-and-network; *c* – subboundaries.

Let us compare the results of the temperature and creep processes. As can be seen from Table 1, 900°C annealing during 1143 h has no significant effect on the volume fraction of phases in the total volume. Thus, in the initial state this volume fraction is 99.7% (80.0% γ′-phase + 19.7% γ-phase) and after annealing it is 99.5% (83.0% γ′-phase + 16.5% γ-phase). The volume fraction of the ordered γ′-phase slightly increases, while that of the disordered γ-phase slightly decreases. Notably, instead of the secondary χ-phase we observe the secondary $AlRe_2$ phase.

Creep tests show that the phase composition changes both qualitatively and quantitatively. When the alloy state changes from the initial to the post-creep state, the volume fraction of major phases does not change, *i.e.* 99.8% (69.0% γ′-phase + 30.8% γ-phase). Notably, instead of the secondary χ-phase we observe the secondary Laves phase and σ-phase.

It is found that both annealing and creep processes are accompanied by the changing phase composition of secondary phases. During the annealing process, χ-phase dissolves and forms rhenium aluminide. The creep process causes the formation of σ-phase and Laves phase, $AlRe_2$ phase not being observed. The ratio between the volume fractions of γ′- and γ-phases shifts toward the increase in the disordered γ-phase. We, therefore, observe a slight disorder of Re-alloyed superalloy after its long-term thermal treatment. We assume that during the creep process, the localized regions in γ′-phase subjected to thermal treatment become low-stable relative to the order–disorder transfer. As a result, it is that regions that increase the amount of the FCC solid solution in the post-creep state of the alloy.

Dislocation structure

In γ′- and γ-phases, dislocations are observed in each state of the superalloy. Dislocations form mostly network or cell-and-network structure as shown in Fig. 6*a*, *b*. In post-creep states, the formation of subboundaries occurs (Fig. 6*c*)

In specimens, the scalar dislocation density ρ ranges from $11 \cdot 10^{10}$ to $8.5 \cdot 10^{11}$ cm^{-2} in the disordered γ-phase and from $2.5 \cdot 10^{10}$ to $7.5 \cdot 10^{10}$ cm^{-2} in the ordered γ′-phase. This means that the deformation processes occur during both the creep and annealing processes. Usually, the dislocation density in the disordered γ-phase is sometimes several times higher than in the ordered γ′-phase. And the deformation process is therefore more intensive in the disordered γ-phase.

The annealing process results in the natural reduction in the dislocation density of γ- and γ′-phases as shown in Fig. 7, curves *1* and *3*, respectively. During annealing, the dislocation density in γ-phase is higher than in γ′-phase. Thus, the increase in the annealing time results in the reduction in the dislocation density both in γ- and γ′-phases.

As can be seen from Fig. 7, during the creep process the behavior of the scalar dislocation density $\rho = \rho(t)$ in both phases is different (curves *2* and *4,* respectively). The deformation processes are more intensive in the disordered γ-phase. At the same time, the dislocation density in γ′-phase is unchanged. This can be explained by the formation of the localized low-stable regions in γ-phase during the creep test that promotes the formation of the diffusion creep mechanisms just in the disordered γ-phase [6].

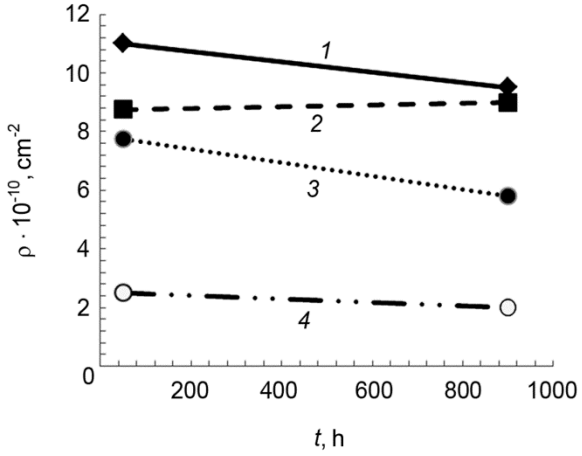

Fig. 7. Scalar dislocation density in γ-phase (curves *1, 2*) and γ′-phase (curves *3, 4*) depending on the annealing (curves *1, 3*) and creep (curves *2, 3*) processing.

CONCLUSIONS

Summing up the experimental results, it can be concluded that the rhenium alloying of Ni–Al–Co superalloy caused the localized transfer of the crystal lattice to the low-stability state. That transfer was accompanied by serious changes in the structure and phase composition of the alloy which were manifested in the appearance of secondary phases, such as σ-phase, χ-phase, Laves phase.

The consequent annealing and creep tests did not affect the phase composition of the alloy, but changed the shape of quasi-cuboids of γ′-phase.

TEM observations showed the formation of different substructures. It was found that the value of the scalar dislocation density in the disordered γ-phase was higher than in the ordered γ′-phase. That indicated to more intense deformation processes in γ-phase.

REFERENCES

1. S. B. Maslenkov, Refractory and High Temperature Resistant Materials. Physicochemical Principles of Creation [in Russian], Nauka, Moscow (1984), p. 15.
2. E. N. Kablov, N. V. Petrushin, and E. S. Elyutin, Vestnik MGTU im. N. E. Baumana. Ser. Mashinostroenie, 38–52 (2011).
3. B. A. Grinberg and M. A. Ivanov, Ni_3Al and TiAl Intermetallic Compounds: Microstructure, Deformation Behavior, Ural Branch of the Russian Academy of Sciences, Ekaterinburg (2002).
4. Ch. T. Sims, N. S. Stoloff, and W. C. Hagel, Superalloys II [Russian translation], Metallurgiya, Moscow (1995).
5. K. B. Povarova, A. A. Drozdov, N. K. Kazanskaya, and A. E. Morozov, Metals, No. 5. 58–71 (2006).
6. Yu. R. Kolobov, E. N. Kablov, E. V. Kozlov, *et al*., Structure and Properties of Intermetallic Compounds with Nanophased Hardening [in Russian], MISiS, Moscow (2008).
7. E. V. Kozlov, A. N. Smirnov, E. L. Nikonenko, *et al*., Phase Morphology and Transformations at Thermal Treatment of Ni–Al–Cr and Ni–Al–Co Superalloys. Scale-Level and Concentration Effects. Innovational Engineering [in Russian], Moscow (2016).

8. E. V. Kozlov, N. A. Koneva, N. A. Popova, and E. L. Nikonenko, Bulletin of the Russian Academy of Sciences: Physics, **72**, No. 8, 1029–1032 (2008).
9. R. C. Reed, The Superalloys – Fundamentals and Applications, University Press, Cambridge (2006).
10. E. L. Nikonenko, N. A. Popova, T. V. Dement, and N. A. Koneva, Russ. Phys. J., **60**, No. 2, 231–235 (2017).
11. A. I. Potekaev, M. D. Starostenkov, and V. V. Kulagina, The Influence of Point and Planar Defects on Structure and Phase Composition of Pre-Transition Low-Stable Region of Metal Systems [in Russian], NTL, Tomsk (2014), 488 p.
12. N. A. Koneva, L. I. Trishkina, A. I. Potekaev, and E. V. Kozlov, Structure and Phase Transformations in Low-Stability States of Metal Systems at Thermal Treatment [in Russian], NTL, Tomsk (2015).
13. P. A. Chaplygin, A. I. Potekaev, A. A. Chaplygina, *et al*., Russ. Phys. J., **58**, No. 4, 485–491 (2015).
14. V. V. Kulagina, A. I. Potekaev, A. A. Klopotov, and M. D. Starostenkov, Russ. Phys. J., **55**, No. 4, 353–361 (2012).
15. A. I. Potekaev, A. A. Klopotov, A. N. Matyunin, E. S. Marchenko, V. E. Gyunter, and Sh. A. Dzhalolov, J. Adv. Mater., **2**, No. 4, 387–394, (2011)
16. I. A. Kurzina, A. I. Potekaev, N. A. Popova, *et al*., Russ. Phys. J., **61**, No. 4, 715–721 (2018).
17. A. I. Potekaev, A. A. Klopotov, V. V. Kulagina, M. D. Starostenkov, *et al*., Steel Transl., **46**, No. 6, 365–369 (2013).
18. A. A. Klopotov, A. I. Potekaev, E. V. Kozlov, and V. V. Kulagina, Russ. Phys. J., **54**, No. 9, 1012–1023 (2012).
19. V. E. Guenther, A. I. Potekaev, A. A. Klopotov, and Yu. E. Grischenko, Russ. Phys. J., **54**, No. 5, 569–575 (2011).
20. A. I. Potekaev, A. A. Klopotov, E. V. Kozlov, and V. V. Kulagina, Low-Stable Pre-Transition Structures in Nickel and Titanium [in Russian], NTL, Tomsk (2004).
21. A. I. Potekaev, A. A. Chaplygina, P. A. Chaplygin, *et al*., Russ. Phys. J., **60**, No. 10, 1776–1786 (2017).
22. F. R. N. Nabarro and H. L. Villiers, The Physics of Creep – Creep and Creep-resistant Alloys, CRC Press, London (1995).
23. H. Mughrabi, Mater. Sci. Technol., **25**, No. 2, 191–204 (2009).
24. T. Murakumo, T. Kobayashi, Y. Koizumi, and H. Harada, Acta Mater., **52**, No. 12, 3737–3744 (2004).
25. Y. Ro, Y. Koizumi, and H. Harada, Mater. Sci. Eng. A, **223**, No. 1–2, 59–63 (1997).
26. C. M. F. Rae and R. C. Reed, Acta Mater., **49**, No. 19, 4113–4125 (2001).
27. T. Sugui, W. Minggang, L. Tang, *et al*., Mater. Sci. Eng. A, **527**, 5444–5451 (2010).